Geophysical Journal International

Geophys. J. Int. (2021) **225,** 1174–1191
Advance Access publication 2020 December 10
GJI Geodynamics and Tectonics

doi: 10.1093/gji/ggaa582

Geological effects and tectonic environment of the 26 November 2019, M_w 6.4 Durres earthquake (Albania)

Eutizio Vittori,[1] Anna Maria Blumetti,[1] Valerio Comerci,[1] Pio Di Manna,[1] Luigi Piccardi,[2] Dashamir Gega[3] and Ismail Hoxha[4]

[1]*Geological Survey of Italy –Higher Institute for Environment Protection and Research (ISPRA), via Vitaliano Brancati,* 48, 00144 *Rome, Italy. E-mail: tizianovittori@gmail.com*
[2]*Istitute of Geosciences and Earth Resources – CNR, Florence, Italy*
[3]*Geological Survey of Albania, Tirana, Albania*
[4]*Institute of Geosciences, Energy, Water and Environment (IGEWE), Polytechnic University of Tirana, Albania*

Accepted 2020 December 3. Received 2020 November 22; in original form 2020 May 28

SUMMARY

The M_w 6.4 26 November 2019, earthquake has been the strongest in the last decades in Albania, causing damages of intensity VIII to IX EMS in the epicentral region around Durres. The region north of Durres has experienced a maximum uplift of *ca*. 11 cm, based on SAR interferometry, which represents the main environmental effect induced by the earthquake. Other coseismic environmental effects were liquefaction mostly in the coastal area north and south of Durres, lateral spread in the Erzen river banks and possibly minor rock falls. As a whole, the observed effects are indicative of an intensity VIII to IX in the ESI scale. The rupture parameters that best fits the earthquake data (seismic moment, hypocentre depth, GPS data, deformation field from SAR interferometry), based on Coulomb modelling, show a reverse slip of 0.6 m on a NW–SE trending plane dipping 25° northeast, 20 km long and *ca*. 12 km wide, from 19.5 to *ca*. 15 km deep. The surface projection of the upper tip of the rupture is on the coast north of Durres. The inferred Coulomb stress change does not impose any significant load on the surrounding major faults, that is Kruja thrust, Lezha transfer fault, and the offshore thrust fault responsible for the 1979 M_w 7.1 Montenegro earthquake. The historical earthquakes and the regional tectonic setting, dominated by plate collision and important transfer fault zones suggest that the last earthquake might not be representative of the actual maximum seismic and surface faulting hazards in northwestern Albania, a region of fast industrial and touristic growth. This calls for detailed active tectonics studies with a palaeoseismological perspective in the region surrounding the epicentral area, where the two main towns in Albania lie.

Key words: Radar interferometry; Europe; Earthquake hazards; Seismicity and tectonics; Tectonics and landscape evolution.

1 INTRODUCTION

Albania lies on the south-westernmost part of the actively convergent boundary between the Eurasian Plate and the Adriatic microplate (Fig. 1). Compressive tectonics, with active shortening in the southwest direction and northwest striking thrusts and folds, dominates especially the external, coastal, areas. On the early morning (02:54 UTC) of 26 November 2019, a M_w 6.4 (IGEWE, EMSC) earthquake hit the northwest of Albania (Durres and Tirana regions), with its epicentre in the coastal area north of Durres, preceded by two rather strong foreshocks on 21 September 2019 (M_w 5.7 and 5.1, IGEWE, EMSC, Ganas *et al.* 2020; Papadopoulos *et al.* 2020). It was felt in a large area extending from Taranto (Italy) to Belgrade (Serbia) and Greece. The earthquake, one of the strongest events to have hit Albania over the last 100 yr, produced heavy damage mainly in Durres, the second biggest town in Albania, Thumana and their surroundings, reaching an epicentral intensity (IGEWE 2019) of degree IX in the EMS-98 scale (Grünthal 1998). Fifty-one people lost their lives and about 3000 were injured.

About 2 weeks after the main shock, a reconnaissance team from the Italian Geological Survey and the CNR (National Research Council) visited the epicentral area, together with colleagues from the Institute of Geosciences, Energy, Water and Environment (IGEWE) and the Albanian Geological Survey to gather data on the geological effects induced by the event. The collection of the effects induced on the natural environment allows to estimate the macroseismic intensity field of the earthquake by applying the Environmental Seismic Intensity scale (ESI2007, Michetti *et al.* 2007;

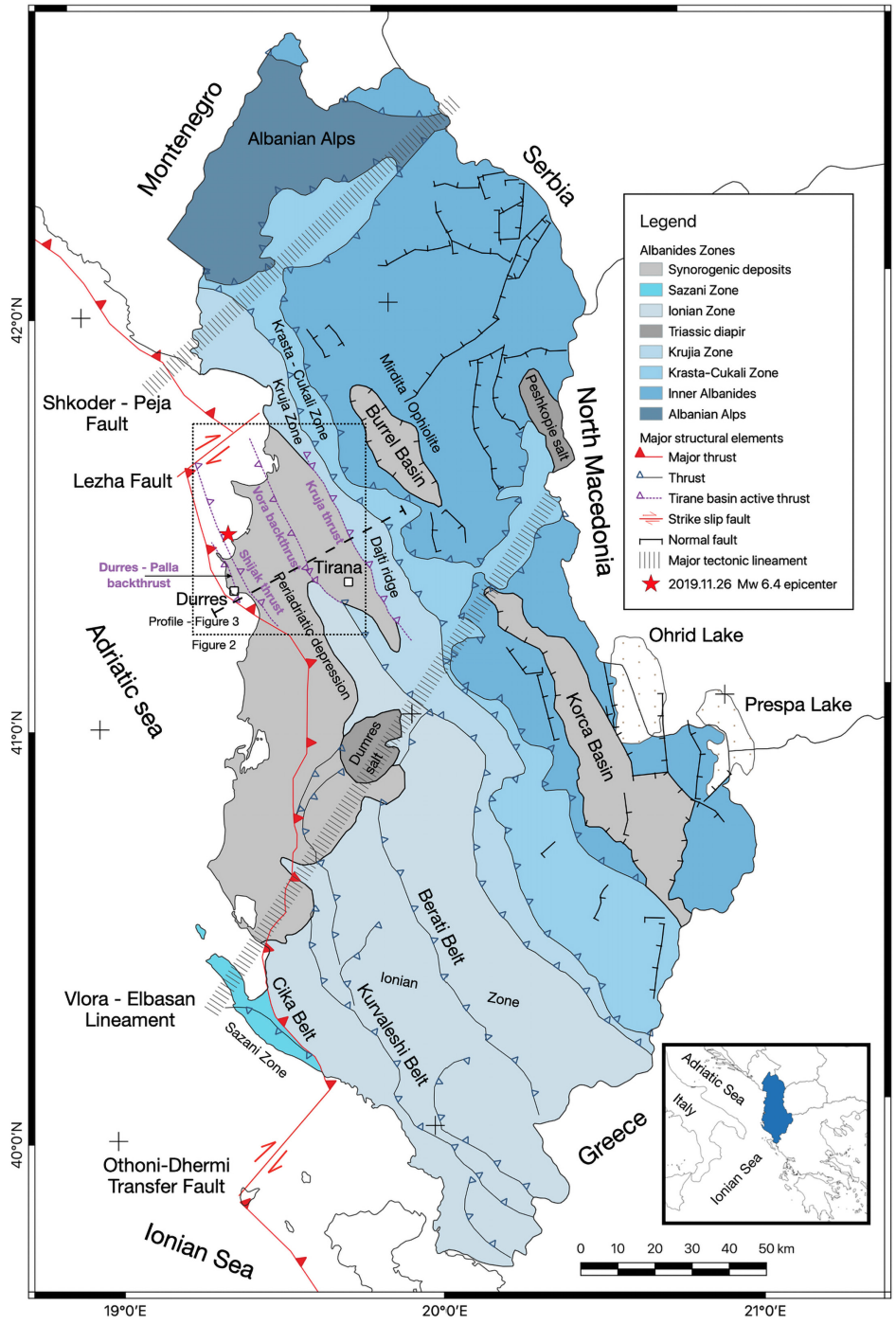

Figure 1. Geological map of Albania with indicated the main tectonic zones and lines. Modified after Velaj *et al.* (1999), Aliaj (2000), Aliaj *et al.* (2004), Roure *et al.* (2004), Hoffmann *et al.* (2010), Reicherter *et al.* (2011), Jouanne *et al.* (2012), Bega (2013a,b), Guzman *et al.* (2013) and Bega & Soto (2017),

Serva *et al.* 2016). This estimate can be compared with the intensity values obtained by applying other scales (e.g. EMS-98) in order to obtain a more substantiated and complete macroseismic evaluation.

The question about the seismogenic potential and capability of the grid of faults mapped in northwestern Albania (Aliaj 2000; Aliaj *et al.* 2004) cannot be addressed here. In addition to the seismological and GPS data, there is geomorphological evidence of Late Quaternary and Holocene faulting and folding deformation (Piccardi *et al.* in preparation) that requires a coordinated effort for a palaeoseismological characterization of the region.

There is a special interest in the seismic activity of western Albania also for its relevance in the seismic and tsunami hazard assessment for the overlooking Southern Italy Adriatic regions and the other eastern Adriatic-Ionian facing countries. Moreover, according to some authors, there is evidence of a direct correlation between seismicity in Albania and in the southern Adriatic sector of Italy (e.g. Mantovani *et al.* 2010; Viti *et al.* 2015, and references therein),

possibly due to the rigid motion of the Adria–Apulia microplates (e.g. D'Agostino *et al.* 2008) that connect both sides of the southern Adriatic Sea.

2 REGIONAL SETTING

2.1 Stratigraphy and tectonics overview

The Albanides mountain belt is a segment of the Dinarides–Hellenides orogen, originated by the initial NE subduction of the Adriatic–Apulian–Ionian microplate under the Eurasian Plate and their subsequent continental collision (Aubouin *et al.* 1970; Doglioni 1991; Kilias *et al.* 2001; Doglioni *et al.* 2007; Schmid *et al.* 2008; Biermanns *et al.* 2018; Handy *et al.* 2019; Schmid *et al.* 2019). Subduction roll-back and slab retreat started since the Early Miocene shaping the structures of the Dinarides–Hellenides belt and deforming its foreland (Hoffmann *et al.* 2010; Handy *et al.* 2019). Presently, slab break-off seems to be the dominant process responsible for the compressional stress regime in the Dinaric–Hellenic front (Dumurdzanov *et al.* 2005; Hoffmann *et al.* 2010; Biermanns *et al.* 2018, and references therein).

The NW–SE trending Albanides mountain belt represents a typical SW-verging fold and thrust belt system (De Celles & Giles 1996) showing different structural organization and timing of deformation along the verging direction. Two main tectonic domains are identified: (i) the Internal or Eastern Albanides, consisting of metamorphic sequences, in particular the Jurassic ophiolites of the Mirdita suture zone of the Tethys Ocean with a thick-skinned thrust sheets architecture (Velaj *et al.* 1999; Roure *et al.* 2004) and (ii) the External or Western Albanides characterized by Triassic to Eocene carbonates and Oligocene to Pliocene siliciclastic deposits, show a prevalently thin-skinned structural setting with the main thrust units detached on top of the Triassic evaporites (Roure & Sassi 1995; Veija *et al.* 1999; Meço & Aliaj 2000; Roure *et al.* 2004; Jardin *et al.* 2011; Naço *et al.* 2014; Veja 2015a,b; Bega & Soto 2017; Fig. 1).

The External Albanides include three main tectonic zones, from east to west, Krassta-Cukali, Kruja and Ionian, delimited by thrust faults named after them (Roure *et al.* 1995a,b, 2004; Velaj *et al.* 1999; Velaj 2015a,b; Bega & Soto 2017).

Two major NE–SW trending strike slip structures interrupt the continuity of the thrusts units controlling the sedimentary and tectonic evolution of the Albanides. In northern Albania, the Shkodra-Peja Fault Zone separates the Albanides from the Albanian Alps and the Dinarides (Fig. 1). To the south, the SW–NE-trending Vlora–Elbasan lineament (e.g. Roure *et al.* 2004, Lacombe *et al.* 2009) roughly marks the boundary between the Ionian and the Adriatic sectors of the External Albanides. A large foredeep basin (Periadriatic Depression) extends northward from the Vlora–Elbasan lineament filled with Oligocene to Quaternary siliciclastic terrigenous deposits more than 6 km thick. Southward, the Sazani Zone, that is the easternmost remain of the Apulian Mesozoic platform (foreland) crops out (Roure *et al.* 1995a,b; Velaj *et al.* 1999; Nikolla *et al.* 2002; Roure *et al.* 2004; Velaj 2015a).XXX

A relevant role in the regional structural setting of the northern Albanides might be played also by the right-lateral Lezha fault zone, parallel to the Shkodra–Peja Fault Zone (Xhomo *et al.* 1999; Aliaj *et al.* 2000, 2004; Hoxha 2020, Figs 1 and 2). This transverse lineament separates inland two Plio-Quaternary thrust and fold belts of different axial orientation: about NW–SE in the north (Dinarides trend) and about NNW–SSE to the south. Moreover, across the Lezha fault a rapid change of the GPS velocity field occurs (Jouanne *et al.* 2012).

Geophysical data indicate that the depth of the Moho increases from 25–30 km under the Adriatic to 40–50 km under the axial zone of the Albanides (Grad *et al.* 2009; Frasheri *et al.* 2009; Handy *et al.* 2019; Stipcevich *et al.* 2020). In general, the depth of the seismogenic layer tends to follow the shape of the Moho and, based on Stipcevic *et al.* (2020), is constrained to the upper crust, since most seismic events have hypocentral depth within 10 km in the northern Adriatic eastern coast deepening to 20 km in the southern tip of the Croatian coast.

2.2 Current tectonic style in northwestern Albanides

There is ample evidence of the frontal thrust that runs offshore Montenegro, across the lowlands of Albania, continuing in western Greece to connect with the Hellenic subduction (e.g., Kiratzi & Dimakis 2013, Fig. 1). Its Adriatic-Ionian sector, north of the Cephalonia transform fault, despite the lack of an active subduction, is still undergoing shortening, as proven by its tectonic style, GPS monitoring (e.g. D'Agostino *et al.* 2008; Jouanne *et al.* 2012), and intense seismicity. A recent proof of the latter was the M_w 7.1 Montenegro (Ulcinj) earthquake of 1979 (e.g. Benetatos & Kiratzi 2006). Ormeni *et al.* (2013) corroborate the activity of the Adriatic Sea deep crustal fault zone at the border between the Adriatic Sea platform and the orogen highlighting that the 21 August 2009 Adriatic Sea earthquake ($M_w = 5.6$) was generated by the reactivation of a NW-trending reverse fault (N22W) in the Ulcinj zone.

Handy *et al.* (2019) show the trace of the basal thrust system of the Kruja and Ionian zone and its southward prolongation in the Hellenic region, highlighting displacement and clockwise rotation of the Hellenic area with respect to the Albanides as a consequence of a different rate of rollback subduction. The basal thrust of the Kruja unit is represented blanketed by deformed Miocene terrigenous deposits in Velaj (2011). Currently, Internal and External Albanides are characterized by different tectonic regimes (Aliaj *et al.* 2004; Hoffmann *et al.* 2010; Jouanne *et al.* 2012; Kiratzi & Dimakis 2013). The thrust sheets of the Internal Albanides are undergoing extension and uplift, being overprinted by a Plio-Quaternary system of horst and graben that make a kind of Basin-and-Range architecture (Hoffmann *et al.* 2010, Guzmán *et al.* 2013; Ormeni *et al.* 2013). Relevant local east-west to N160° extension affected the Korca and the Ohrid active grabens at the boundary between Albania–North Macedonia and Greece (Jouanne *et al.* 2012). Instead, the External Albanides and the foredeep, westward from the Kruja zone, are still undergoing shortening with active SW-verging folding and thrusting and passive NE-verging roof thrust largely involving the foredeep deposits (Roure *et al.* 2004; Aliaj *et al.* 2004; Jouanne *et al.* 2012; Bega 2013b; Bega & Soto 2017).

GPS monitoring shows that the shortening increases from north to south with a progressive change in the shortening direction from east-west in northern Albania to N80°E in the south. Major changes in the velocity field reflect the location of major active transverse zones: the Shkoder-Peja fault zone, the Lezha fault, the Othoni-Dhërmi transfer fault (Jouanne *et al.* 2012).

The Shkoder–Peja fault is a major NE–SW transverse active fault that affects the whole collision belt. Instead, the Lezha and the Othoni–Dhërmi faults seem to affect only the external Albanides (Jouanne *et al.* 2012). The Lezha fault is a poorly known transfer structure that dextrally offsets in northern Albania the frontal Neogene–Present thrust wedge (Handy *et al.* 2020).

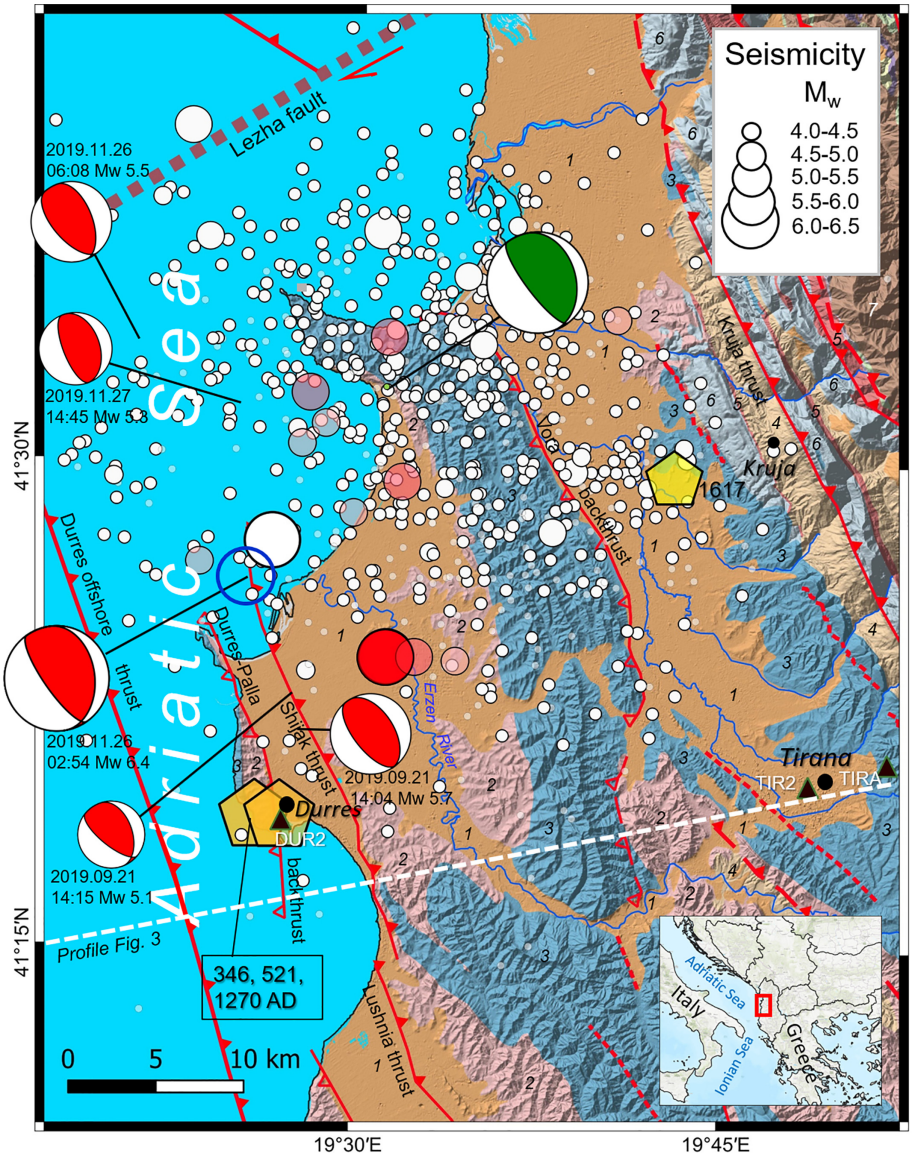

Figure 2. Location of the 26 November 2019, earthquake. The epicentre according to INGV (red), NEIC (empty blue) and IGEWE (green) are shown, together with the aftershocks (white circles) recorded until January 2020 (IGEWE); size proportional to magnitude as in box in upper right. In colour are the aftershocks recorded by the ISIDE network (INGV). Pentagons locate the historical earthquakes of 346 AD (M_e 6.6, I X–XI), 521 (M_e 6.2, I IX–X) and 1270 (M_e 6.2, I IX–X) (CFTI, Guidoboni *et al.* 2019), 1617 (M 6.2, I VIII MSK, Sulstarova & Kociu 1975). The focal mechanisms (according to RCMT catalogue, Pondrelli 2002) of the main shocks of the sequence ($M_w > 5.0$) show a consistent reverse fault rupture with NW–SE strike; in green, the very similar but more northerly solution of the main shock from IGEWE. Beachball sizes proportional to indicated magnitude. Black triangles: GPS stations. Dotted white line is the trace of profile of Fig. 3, which extends slightly beyond the margins of the figure. Background colours according to the online Geological Map of Albania (https://geoportal.asig.gov.al/en/data) draped on the ALOS DTM (30 m resolution): 1 Alluvial-proluvial sediments (Pleistocene to Holocene); 2 Clays to sandstones, conglomerates (Middle-Early Pliocene); 3 undifferentiated sandstones, claystones, limestones (Late Miocene) and evaporites (Messinian); 4 Flysch deposits and limestones (Oligocene); 5 Red marls, siltstones (Paleocene-Eocene); 6 Shelf limestones (Late Cretaceous); 7 Ultramafic igneous rocks: harzburgite-lherzolites with rare dunite (Middle Jurassic).

The northern coastal region, where the November 2019 earthquake originated, is crossed by a number of seismic lines for its hydrocarbon potential. They provide a valuable, but somehow still controversial, representation of the fold and thrust system. In fact, the various sections (Skrami 2001; Roure *et al.* 2004; Aliaj 2006; Lacombe *et al.* 2009; Aliaj *et al.* 2010; Bega 2013a; Velaj, 2011, 2015a,b; Lule & Nazaj 2020) show the complexity of the northern Albanian thrust front, dominated by the interaction between the Kruja Zone and its westward deformed foredeep (Peri-Adriatic domain) and Apulian foreland. Moreover, the seismic lines do not reach deep enough to portrait the major seismogenic structures at the foot of the pile of thrust sheets. According to several authors, a regional scale triangle zone developed during Pliocene-Quaternary times in the overthrust front of the Kruja duplex, probably as a result of the interaction of compressional processes and extensional high-angle structures inherited from the former Tethyan passive margin (Aliaj *et al.* 2004; Roure *et al.* 2004; Aliaj 2006; Bega 2013a,b). The interpreted geological profiles in Fantoni & Franciosi (2010) and Argnani (2013) show this triangle as a deep wedging of the west-verging thrusts that causes the ramping of backthrust

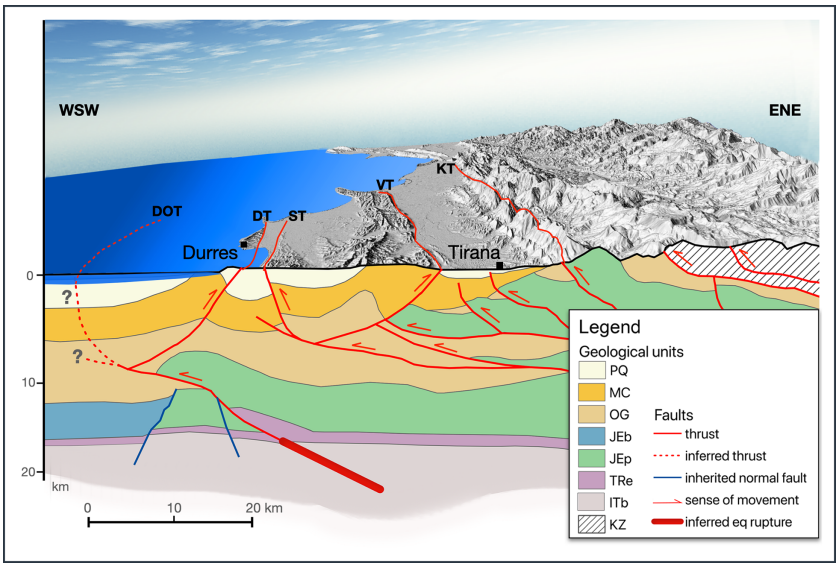

Figure 3. Schematic, highly speculative, section across the 2019 earthquake region, modified after Roure *et al.* (2004), Aliaj (2006) and Bega (2013a) (trace in Fig. 1 and Fig. 2). Considering that the deep structure is poorly documented by seismic lines, the rupture zone may actually run along the contact between the Trias evaporites and the metamorphic basement. The shallower geometry of the frontal thrust zone under Durres and in the offshore area (left in figure) is also poorly constrained. It may cut through the Miocene to Quaternary layers, or make a flat westwards. PQ, Pliocene–Quaternary; MC, Miocene terrigenous sediments; OG, Oligocene terrigenous sediments; JEb, Jurassic–Eocene carbonates (Albanian basin); JEp, Jurassic–Eocene carbonates (shelf platform); TRe, Triassic evaporites; ITb, Infra-Triassic basement; KZ Krasta Zone (ultramafic rocks).

structures. Deep thrusts push up and westward the rigid pile of the Jurassic–Eocene shelf carbonate deposits acting as a wedge under the Oligocene–Miocene terrigenous succession on which passive east-verging thrusts grow-up, thus explaining why only the latter appear to cut the sea bottom. Fig. 3 tries to combine in a synthetic, highly speculative, section trending ENE–ESW several published profiles running across, or close to, the earthquake zone, especially the profiles found in Roure *et al.* (2004), Aliaj (2006) and Bega (2013a). As already pointed out, the deeper structure is not imaged by seismic lines and the geometry of the basal thrust, especially in the offshore area, is quite poorly constrained.

The SW-verging Kruja thrust system constitutes a major stack of duplexes, but in its frontal zone backthrusting and triangular zones increase the complexity of the structural mosaic. A prominent NE-verging thrust appears locally to overprint the SW-verging thrust sheet, opening a question on the identification of the major seismic sources and the role and the seismic potential of the backthrusts. Bega (2013) has identified two main NE-verging thrusts, the Preza (or Adriatic–Krraba) backthrust (here named Vora backthrust), separating the Tirana and the Shijak basinsand the Durres–Palla backthrust bounding to the east the Durres hills (Figs 1and 2). According to Bega (2013, and references therein) both backthrusts are to be interpreted as passive roof thrusts: the development of the Vora thrust is due to the westward motion of the buried platform carbonate wedges of the Kruja unit. The Durres–Palla backthrust is due to a combination of stepping geometry between pelagic and platform carbonates and of a westward higher Plio-Miocene subsidence. Its northern prolongation appears to join the triangular zone described by Roure *et al.* (2004) and Aliaj (2006).

The DISS and SHARE projects catalogue the main Albanides frontal thrust and the major back-thrusts as seismogenic sources. From east to west, they are: Kruja thrust; Vora backthrust; Shijak thrust and Lushnia thrust. In part, these seismic sources coincide with the active faults mapped by Aliaj (2000) and Aliaj *et al*. (2004, 2010); however, in these papers the frontal thrusts do not appear to have now any major role. The name ‘Lushnia’ for the thrust offshore Durres is possibly confusing with the Lushnia thrust of Aliaj (2000), so here it is named Durres offshore thrust (Fig. 2). In Fig. 1, this thrust is linked to a thrust running onshore, since there is no geological knowledge in the literature of a thrust system continuing offshore to the south. However, the existence of such an offshore thrust is likely, maybe a blind structure, because of the widespread deformation in the synorogenic foredeep deposits.

Thus, the main active faults in the source area of the 2019 earthquake are (Fig. 2): Lezha fault, Kruja thrust, Vora backthrust, Shijak and Lushnia thrusts, Durres-Palla backthrust, Durres Offshore thrust, the latter corresponding to the surface projection of the frontal thrust of the Kruja–Ionian thrust system.

The seismic potential of the backthrusts is supposedly modest, considering their likely passive role and moderate extension at depth (6–7 km?). Nonetheless, their surface faulting potential cannot be negligible due the possibility of sympathetic motion triggered by, or secondary rupturing related to, major slip events on the west-verging thrusts.

3 HISTORICAL SEISMICITY

The whole Albania is an earthquake country, as proven by its diffuse seismicity, both historical (see in particular the CFTIMed Catalogue, Guidoboni *et al.* 2019; and then Mihalovijc 1951; Karnik 1969; Sulstarova & Kociu 1975; Papazachos & Papazachou 2003; Aliaj *et al.* 2010; SHEEC, Stucchi *et al.* 2013) and instrumental (e.g. IGEWE bulletins, ISC catalogue; Makropoulos *et al.* 2012). In the study region, the earliest known events are all referred to Durres (Dyrrachium or Epidamnos were its Latin and Greek names, Figs 1 and 2). It was a strategic port in ancient times along the via Egnatia route, which connected Roma, through the ports of Brundisium (now Brindisi, on the Italian coast) and Dyrrachium, to Greece and the Middle East. Earthquakes occurred in 58/57 BC (remembered

by Plutarch in his Life of Cicero, 32.4, possibly associated with a tsunami wave), 346 and 521/522 AD. In 346, the city and its walls collapsed entirely, and were rebuilt only four centuries later by Anastasius II 12 m high and so thick that four horsemen could ride them abreast, as reported in the *Alexiad* by Anna Komnene; the estimated intensity MCS was X–XI, corresponding to an estimated magnitude (M_e) 6.6 (CFTIMed). The 521 AD earthquake was somehow smaller but still very damaging (intensity IX–X, M_e 6.2). The next devastating earthquake struck Durres in 1273, described by the Byzantine historian Georghios Pachymeres in his *Relationes historicae* (Elsie, 2003): only the acropolis remained standing and the city was looted and temporarily abandoned. According to CFTIMed, the intensity was IX–X, M_e 6.2, and it occurred in March 1270. Since then, apart from the event of estimated magnitude 6.2 that hit Kruja in 1617 (Sulstarova & Kociu 1975), no major earthquakes were recorded around Durres until the XIX century, when a seismic sequence occurred in 1869–1870 (Mmax 6.5; Sulstarova & Kociu 1975; SHEEC catalogue in Resources section). Another sequence listed in 1894–1896 (Mmax 6.2) by SHEEC is not reported in other catalogues (e.g. Aliaj *et al.* 2010). Several events of $M < 5.9$ occurred in the XX century 20–40 km southeast of the 2019 event (Makropoulos *et al.* 2012). Only the December 1926 earthquake caused severe damage (VIII MSK, M_s 6.0) in Durres, Shijak and southwards (Aliaj *et al.* 2010). Thus, we can observe that two major clusters of seismicity have hit the area, in 346–521 and 1869 to now, separated by an 'isolated' shock in 1270. Thus, there have been two periods of substantial quiescence of 750 and 600 yr, respectively. The last period of clustered activity, began in 1869, has seen other comparable events in 1926 and 2019 and there is no way now to rule out that this sequence can continue in the next years with similar or even larger shocks, similarly to the 346–521 cluster.

The study of the probabilistic seismic hazard in Albania by Aliaj *et al.* (2004) estimates the historical seismic catalogue to be complete for magnitude ≥7 since 1200, magnitude ≥6 since 1800, magnitude 4.5 since 1901. Actually, there are no known earthquakes of magnitude >6.6 in the whole historical catalogue, but the estimated uncertainty is 0.25–0.5. For the region including Durres (PL, Periadric Lowland) and that immediately to the northwest (LU, Lezha-Ulcinj), maximum magnitudes 7.0 and 7.2, respectively, were adopted by Aliaj *et al.* (2004) for the calculations. To the east (EAB, Eastern Albania Background), a background Mmax 6.5 was chosen. High resolution neotectonic studies, see Discussion ahead, are needed to improve this model for the inland seismogenic sources.

4 THE EVENT

4.1 Instrumental seismic data

Different seismological institutes (INGV, IGEWE and NEIC) all constrain the epicentre location of the November 2019 earthquake in the coastal area about 10 km north of Durres (Fig. 2). The IGEWE's and NEIC's epicentres are more or less at the mouth of the Erzen river, while the INGV's is more eastward. The moment magnitude (M_w) has been estimated between 6.2 and 6.4. According to INGV (http://cnt.rm.ingv.it/en/event/23487611), the M_w was 6.2, with a hypocentre depth of 21 km, while IGEWE estimated an M_w 6.4 at a depth of 38 km (https://www.geo.edu.al/newweb/?fq = bota). All the available focal mechanism solutions of the main event and of the fore and aftershocks with $M_w > 5$ (sources RCMT, GCMT, EMSC) show a dominating reverse slip rupture along a fault trending NW–SE to NNW–SSE. The RCMT solutions are represented as red beachballs in Fig. 2. The solution from IGEWE (green beachball in Fig. 2) is shifted several kilometres north compared with the epicentre location of the same seismic network and shallower (18 km versus 38 km). The nodal planes of the RCMT solution for the main shock dip 22° to N81 and 71° to N245. The NNW–SSE strike is in good agreement with the earlier focal mechanisms known for the same region (e.g. Pondrelli 2002). Notably, the main shock was heralded by a strong foreshock on September 21 (M_w 5.5, depth 16 km, according to the IGEWE focal mechanism) with epicentre just north of Durres, hence very close to it and reasonably on the same fault.

Two aftershocks of $M_w > 5$ took place on the same day (06:08 a.m., M_w 5.5) and on the 27th (M_w 5.3). The numerous aftershock hypocentres recorded by the IGEWE seismic network and published in its periodic bulletin (IGEWE 2019) result scattered in a large volume down to 50 km and more under the epicentre, without defining any clear rupture plane. The few hypocentres from the ISIDE (INGV) catalogue are suggestive of an east-dipping plane, but they, as well as those in the ISC catalogue, are insufficient to pinpoint a reliable preferential rupture plane. Thus, the only conjecture might be that of a rupture zone originating quite deep, possibly at the bottom of the upper, brittle, crust (Fig. 4), but very unlikely seismically involving the lower ductile crust, since this would imply a much deeper rupture hardly compatible with the DInSAR data and Coulomb modelling, as shown ahead.

The seismic moment (M_0) from the several focal mechanisms now available (e.g. IGEWE, RCMT, EMSC, ISC and GCMT, see the resources section) ranges between 2.4^{18} N·m (RCMT, M_w 6.2) and 5.6^{18} N·m (GCMT, M_w 6.4). Of the two nodal planes, one dips west quite steeply (49–82°), while the other one dips east with angle 10–29°. The estimated strike varies from N335 (GFZ) to N–S (e.g. IPGP). As a whole, the preferred ruptured fault strikes NNW–SSE, gently dipping east. The estimated hypocentre depth varies from 6 (AUTH) to 26 km (GFZ). Rakes vary from almost purely reverse dip-slip (NEIC) to slightly right-oblique (126°, INGV). Papadopoulos *et al.* (2020) locate the hypocentre at a depth of *ca*. 22 km by modelling *P* and *S* phases, with a reverse slip (rake 99°) along a plane striking 345°N.

4.2 Macroseismic data

A macroseismic field is provided in the IGEWE November Bulletin (IGEWE, 2019) with intensities given in the EMS-98 scale, mostly based on questionnaires. The highest values, IX degree, were felt in villages close to Durres: Hamallaj, Jube, Rrushkull, Thumana. Intensities between VIII and VIII–IX were suffered by several towns, including Durres, where the collapse of buildings caused 25 casualties, Shijak, Vora and Thumana (death toll of 25). The intensity felt in Tirana (1 victim) was VII. A detailed account on the effects of the earthquake is found in Lekkas *et al.* (2019b), who have made a survey of the damaged area soon after the event. They report major damages to buildings in two elliptical areas of unconsolidated sediments and shallow water table, one around Durres and the coastal plain of Hamallaj, close to the instrumental epicentre, and another away from the epicentral zone in the Tirana Valley near Kruja. The distribution of damages is rather uneven, strongly influenced by site effects and type and quality of foundations and construction. Papadopoulos *et al.* (2020) estimate an VIII–IX intensity MM and EMS-98. The Ml 5.6 (M_w 5.7) September 21 foreshock

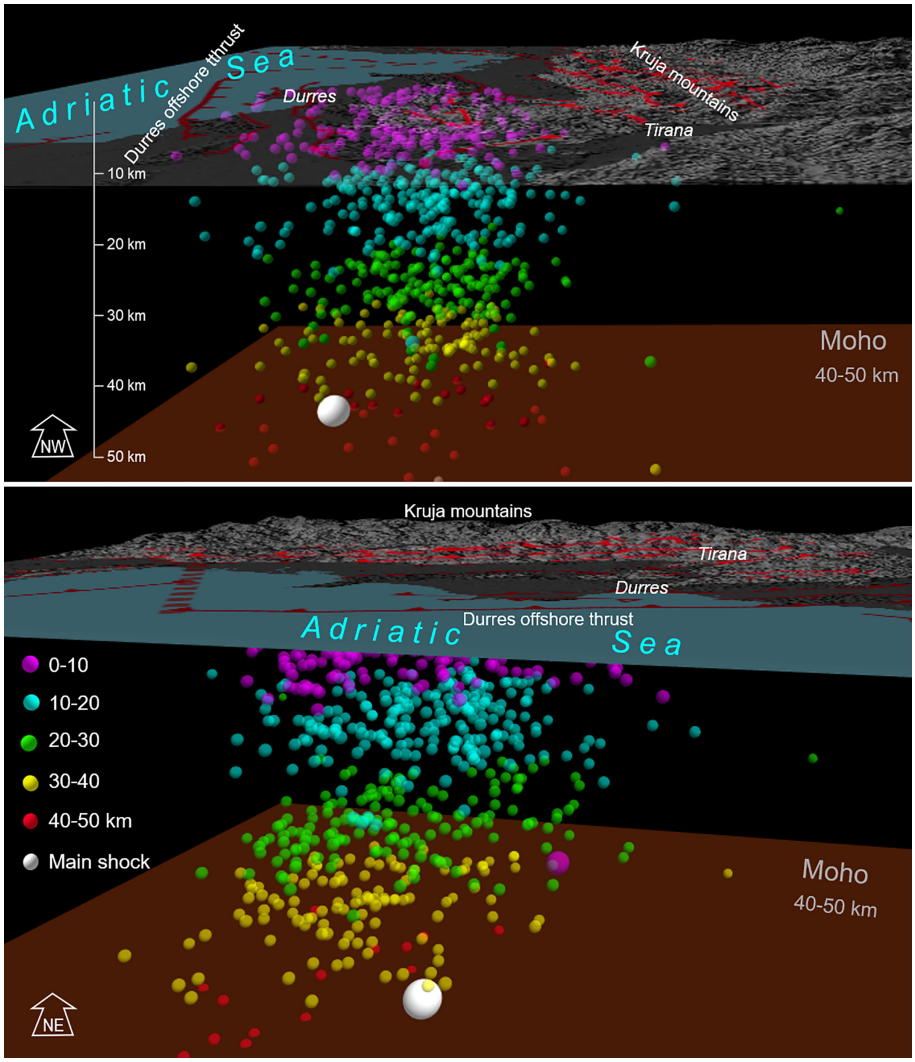

Figure 4. Distribution of all seismic events in the IGEWE bulletins (November 2019 to January 2020). Above: view from southeast parallel to the strike of most fault planes; below: view from southwest orthogonal to main fault structures. No clear rupture planes or trends are discernible. Some hypocentres go deeper than 40 km, the likely bottom of the crust here (e.g. Grad *et al.* 2009). Largest green ball: main shock.

had already caused intensity VIII EMS damages along the coastal region of the Durres District (IGEWE September 2019 Bulletin; Lekkas *et al.* 2019a; Papadopoulos *et al.* 2020). Such earlier damage might have weakened many structures and thus contributed to the damage of November 26.

4.3 Ground deformation pattern and modelling

The preliminary interpretation of the GPS data (http://ring.gm.ingv.it/?*P*=1419; http://147.162.183.197/ALBANIA/; Caporali *et al.* 2020) shows a displacement toward southwest of *ca*. 2.4 cm (1.1 cm of vertical uplift) of the DUR2 (Durres) station, that is the closest to the epicentre. The other few GPS stations are rather far, for example RRES (Rreshen), TIRN and TIR2 (Tirana), and have experienced only negligible millimetric displacement.

A displacement map was obtained here by means of differential interferometry (DinSAR) of radar satellite data, that is Sentinel 1 C band TOPSAR scenes, taken just before (November 25, master scene) and after (December 1) the earthquake, from both descending and ascending orbits. The processing was carried out with the SNAP package of ESA (Braun & Veci 2020). The superficial deformation shows the typical pattern observed in reverse faulting events (Fig. 5, Fig. 6). Three fringes in the ascending interferogram outline a NNW–SSE elongated convex 'bowl' with a maximum uplift of 8–9 cm in the LOS (line-of-sight) direction (estimated from phase unwrapped with the SNAPHU code), centred on the coastal area of Hamallaj, a few kilometres north of the instrumental epicentre. The actual shape of the uplifted zone is only partially known, being its western side offshore. Moreover, the edge effect along the coast influences the unwrapping process, so that also the true uplift cannot be well constrained. Topographic effects and possibly secondary movements complicate the shape of the subsided zone located to the northeast, in the Tirana Valley and the Kruja mountain range.

The uplifted zone marks the hanging-wall of the ruptured fault, without any evident tightening of fringes typically observed where the rupture comes close to the surface. This is likely due to the incomplete portrait of the deformation pattern, about half offshore, and to the depth of the ruptured zone. The inversion from uplift to subsidence occurs just east of the NNW–SSE-elongated system of folds between the Shijak and Tirana basins, bordered by the

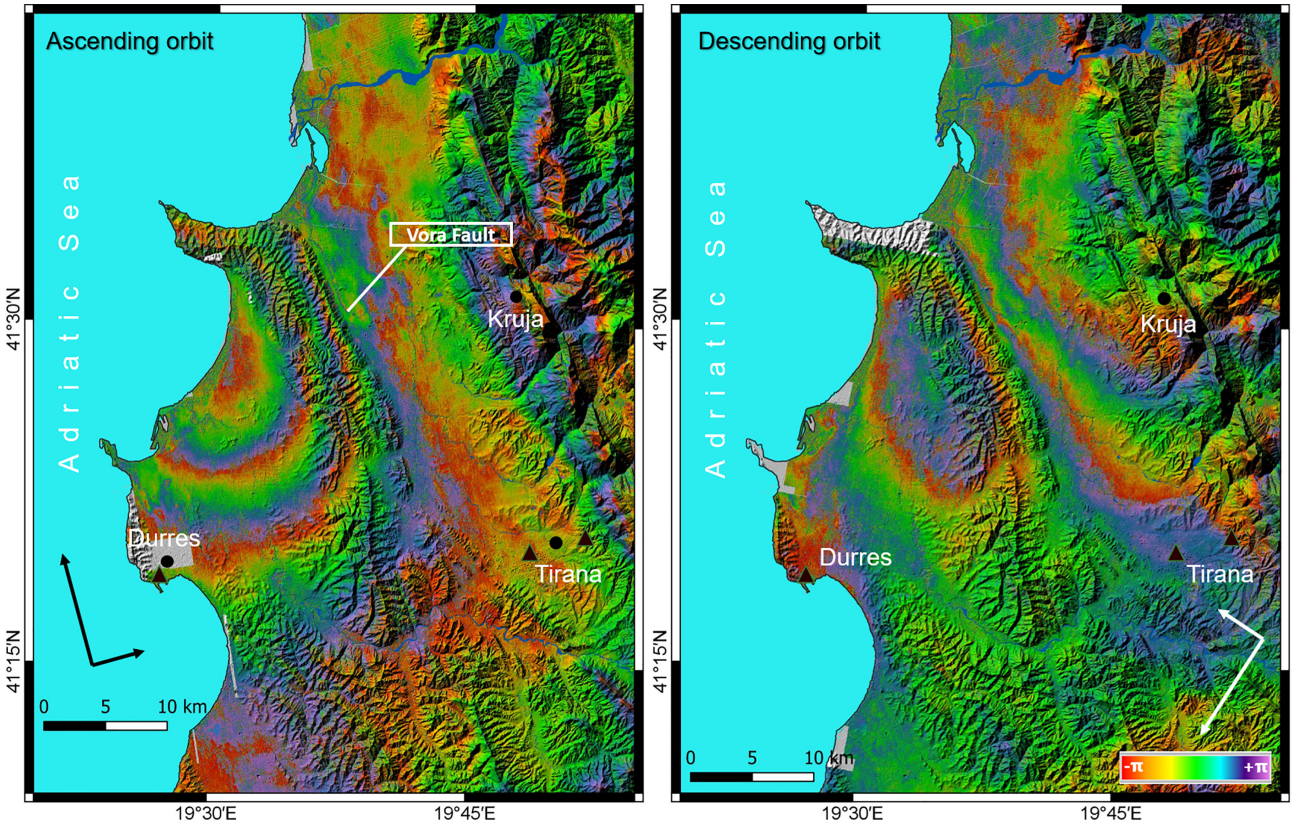

Figure 5. Result of differential interferometry (DinSAR) for the 2019 earthquake (Sentinel 1 TOPSAR SLC scenes taken on November 25, master, and December 1). The distribution of fringes, draped on the DTM from ALOS (resolution 30 m), is better represented in the left figure, because of the more favourable angle of view of the ascending orbit, almost orthogonal to faulting, with respect to the descending orbit (right figure), almost parallel to faulting. Thus, in the descending interferogram only one fringe is well represented and the resulting highest uplift (*ca.* 6 cm) is shifted several kilometres to the northeast. The offshore pattern is unknown; moreover, the abrupt loss of coherence along the coast disturbs the interferogram formation.

active Vora backthrust (Fig. 2). However, as described before in the Regional setting chapter, seismic profiles show that this fault is rather shallow (6–7 km max) so that it could not be the source of the event, which has to be sought in the west-verging major thrust system.

The preliminary attempts at modelling the deformation field appeared soon after the event (https://twitter.com/simoneatzori73/status/1202587167979134976) proved it difficult, also because of the uncertainties in modelling fringes that are only partially known. Caporali *et al.* (2020) have modelled a rather shallow (8 km) thrust plane gently plunging northeast, accounting reasonably well for the southwest movement pointed out by the DUR2 GPS station. A similar conclusion is obtained by Ganas *et al.* (2020), whose inversion modelling indicates a 22 by 13 km rupture on a fault dipping 23° east and top of rupture at 16.5 km of depth.

A modelling of the rupture, also aimed at estimating the influence of this last event on the stress state of the nearby active faults, has been carried out also in the present paper by means of the Coulomb software (version 3.3, Toda *et al.* 2011). The input data have been constrained based on the known geology and the seismological and GPS data cited before. The almost purely compressive focal mechanisms constrain the seismic moment M_0 to range between 2.8 and 5.6 $\times$ 10^{18} N·m (M_w 6.2–6.4): the averaged M_0 would be around 4.5 (M_w 6.4). Of the two nodal planes, the one gently dipping east-northeast is preferred as rupture plane, corresponding to the geometry of the main thrust system, west-verging (see Tectonic Setting chapter ahead). The initial fault position and strike was estimated based on the distribution of hypocentres and surface deformation from interferometry (Fig. 6). The strike value chosen here is N340, which is in agreement with the average strike of the superficial reverse fault traces, with dip 25°. The latter is an average value of the dips obtained in the available focal mechanisms. The focal depth is also estimated as the average value of the available depths to be around 20 km. For a reverse rupture of M_w 6.4, the empirical relationships of Wells & Coppersmith (1994) and Leonard (2014) provide rupture areas of *ca.* 190 (Rupture Length at Depth – RLD – 19.6 km, Width – W – 10.3 km) and 250 km^2 (RLD 20 km for W 12.7 km), respectively. The choice of RLD and W constrains the average slip (D) to 0.6 m through the M_0. The average rake of the available focal solutions is 115°, but the general tectonic setting is suggestive of a stress field orthogonal to the fault strike, thus, rakes 90° and 115° have been tested. The distribution of aftershocks would indicate an RLD in excess of 30–35 km, which however appears to be too long, since the corresponding W would provide excessive rupture area and/or too small D for the M_0. RLD values <30 km appear more reasonable, likely around or slightly above 20 km. According to the GPS data, only the Durres station has registered a clear southwest-ward movement of 2.4 cm and an uplift of *ca.* 1.1 cm. For comparison, based on their finite velocity model, Papadopoulos *et al.* (2020) model the slip distribution in time, obtaining a slip towards NNW reaching on the main patch 1.5 m. Their resulting M_0 is 5.0 $\times$ 10^{18} N·m,

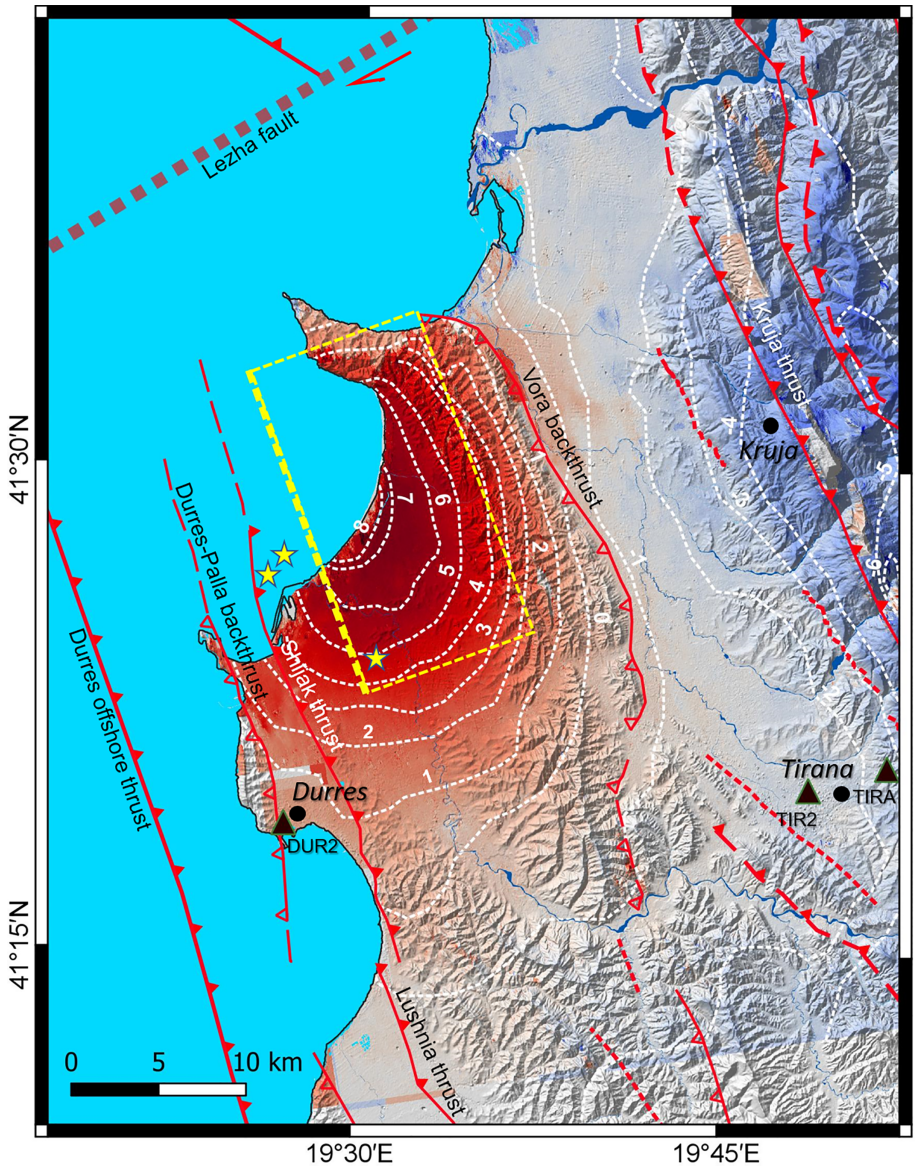

Figure 6. Displacement in the line of sight (LOS) from unwrapping with SNAPHU software, given as red to blue colours (red indicates uplift) and 1 cm contour lines. The coast north of Durres near Hamallaj has experienced a maximum uplift in excess of 8 cm in the LOS. Best candidate as causative seismogenic structure is a SW-verging thrust likely connected to the Durres offshore thrust: see text for details. Yellow dotted line: upper tip of the rupture; box: horizontal projection of the modelled rupture area. Stars: epicentre of the main shock according to different agencies (see Fig. 2). DTM from ALOS (resolution 30 m). Same location of Fig. 2. Black triangles: GPS stations.

Table 1. Fault and rupture parameters used to infer the Coulomb stress change from the 2019 rupture.

Strike	Dip	Rake	RL (km)	W (km)	Slip (M)	Rupture bottom (km)	Rupture top (km)	Resulting M_0 (N·m)
341°N	25° NE	90°	20	11.6	0.6	19.5	14.6	4.44E+18

close to the one adopted in this study for our modelling of rupture (Table 1).

Based on the tectonic setting and the seismological data detailed above, the fault and rupture geometry that best fit the surface deformation in our inversion have the values in Table 1. The fault, whose surface projection of the upper tip of the rupture is just east of the surface trace of the possible offshore prolongation of the Shijak Fault, but much deeper (>14 km), is most likely connected to the Durres offshore thrust (Fig. 6). The latter is represented in the seismic lines described before with a listric geometry, possibly reaching at, or close to, the sea bottom.

The resulting displacement field is given in Fig. 7. The fit with the observed GPS displacement near Durres is good. Less satisfactory is the fit with the other stations, as the Tirana ones, and

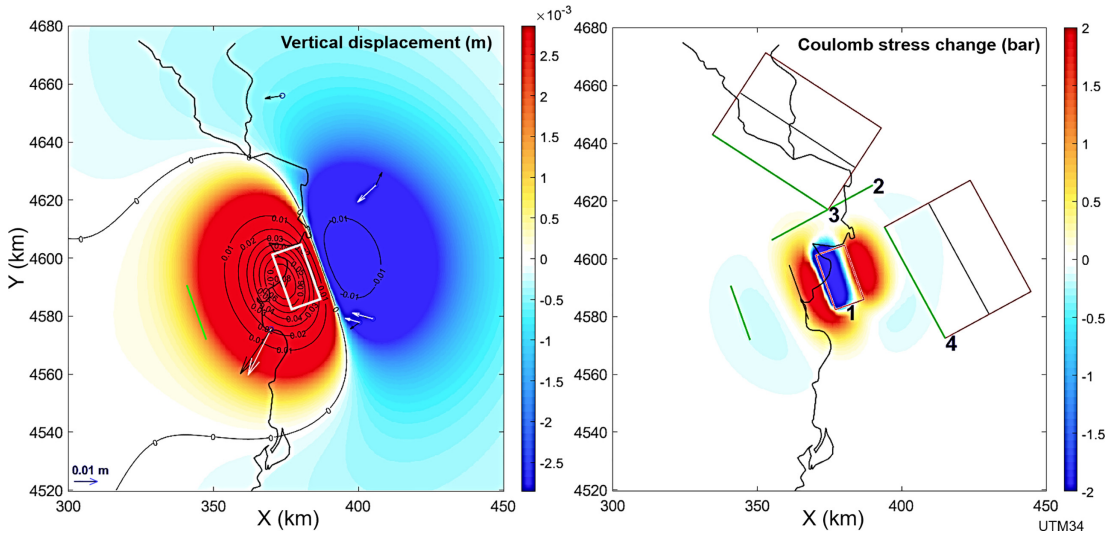

Figure 7. Modelling of the 2019 rupture (Coulomb 3.3, Toda *et al.* 2011). Left-hand panel: distribution of the vertical displacement (arrows are GPS horizontal motions, black measured, white modelled). Right-hand panel: Coulomb stress change induced by the modelled fault rupture. The impact on the most relevant faults nearby is minimal (1 source of the 2019 earthquake; 2: Lezha fault; 3: Montenegro thrust, source of the 1979 M_w 7.1 earthquake; 4 Kruja thrust). Reference system UTM zone 34.

RRES (Rreshen, just outside the northeastern corner of Figs 2 and 5), which however experienced only millimetre wide movements. The modelled displacement is in good agreement in amount and position with that pointed out by the interferometry (compare with Fig. 6). Notably, also the rupture depth fits that suggested by most of the focal mechanisms and hypocentral depths available to now. In comparison, Caporali *et al.* (2020) have estimated a rather shallower source, 8 km deep. One misfit of our model appears to be the more westerly seismological epicentre location, but sources better located with respect to the epicentre would provide large discrepancies with the orientation of the measured horizontal GPS movement and with the location of the maximum uplift in the interferogram and the zone of inversion from uplift to subsidence (east of the Vora backthrust in Fig. 6). Also the introduction of any right lateral component, suggested by several rake angles in the focal mechanisms, would increase the misfit. Our results are in fairly good agreement with those recently obtained by Ganas *et al.* (2020).

Fig. 7 (right-hand panel) shows the Coulomb stress change imposed by the 2019 rupture. It appears to have had a negligible effect on the stress state of the three most relevant faults known in the surroundings: the offshore thrust responsible for the M_w 7.1 Montenegro (Ulcinj) earthquake of 1979 (e.g. Benetatos & Kiratzi 2006), the Lezha right-lateral transfer fault zone and the Kruja thrust, faults described in Section 2.2. Actually, the fault closest to the rupture zone is the Vora backthrust, not modelled here being a quite superficial secondary fault with limited, if any, own seismic potential.

5 EFFECTS OF THE EARTHQUAKE ON THE ENVIRONMENT

The environmental effects associated to earthquakes (EEE—Earthquake Environmental Effects) can be distinguished in two main classes according to the ESI 2007 scale (Michetti *et al.* 2007; Serva *et al.* 2016): primary, that is tectonic deformation, and secondary, that is, induced by seismic shaking. The former includes surface faulting, warping and uplift/subsidence phenomena, which are relevant for both the seismic and the surface faulting hazards. The latter refers to a wide range of geotechnical (slope failures, liquefaction), hydrological (water table and spring discharge fluctuations), physical-chemical (gas emission, change of temperature, etc.) and other (acoustic and light effects, etc.) phenomena. Tsunamis too fall in this category.

A field survey was carried out in mid-December 2019 to map and characterize the environmental effects of the November 2019 sequence, evaluating the extension of the area affected by secondary effects and possibly by primary effects, in order to collect useful data for the future assessment of seismic-related hazards and to apply the ESI scale for the evaluation of the intensity of the earthquake. Under certain geological conditions, for the earthquakes with magnitude above 6, the surface effects are also useful in identifying the seismogenic source. Our surveys focused principally on the southwestern part of the Durres District, closer to the seismic epicentre, and extended to the area around Thumana and, to the north, in the Lezha District (Fig. 8).

5.1 Primary effects

No evidence of primary surface faulting was observed. According to the most widely applied scaling laws (e.g. Wells & Coppersmith 1994; Leonard 2014), the average surface displacement might have been at least 0.5–0.6 m for the given M_w. Being surface rupture also dependent on structural setting, material properties and hypocentre depth, there are several possibly concurring explanations for the lack of a surface rupture inland, first of all, the occurrence of the rupture offshore, despite close to the coast. Second, but not less important, is the deep focal depth, 21 km for INGV and 18 km according to IGEWE's focal mechanism solution, which strongly suggests that the rupture was confined at depth, in agreement with the DinSAR data that shows a rise of the hanging-wall >8 cm (in the LOS) without any tightening of the fringes, and the modelling described in Section 4.3. The field inspection has not pointed out any sign of surface faulting, primary or triggered, along the major faults near the epicentre: the Vora backthrust and the land trace of the Lushnia and Shijak thrusts.

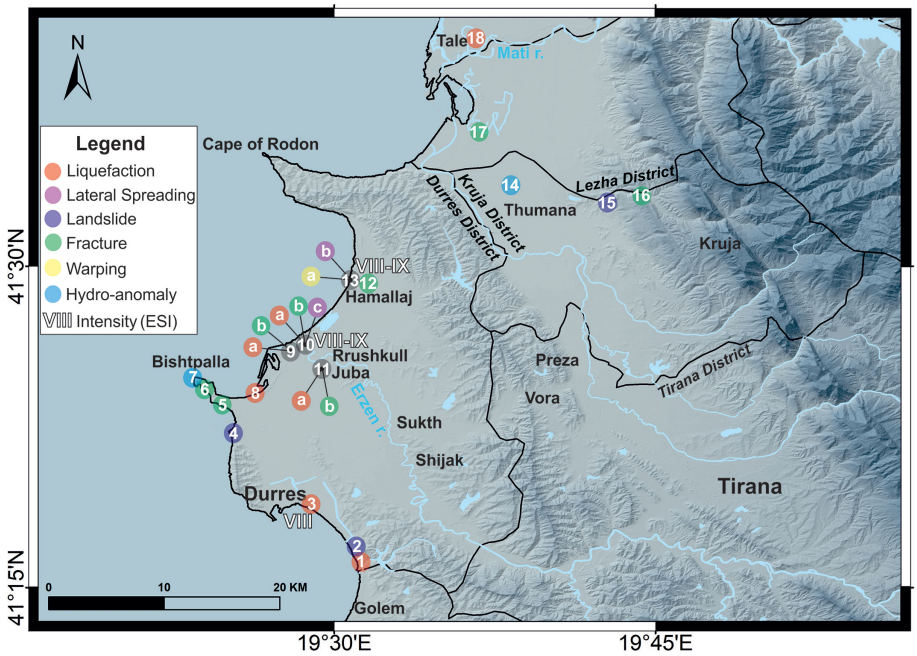

Figure 8. Environmental effects induced by the 26 November 2019, Durres earthquake. Coloured circles show the sites where EEEs have been observed during the field surveys. In sites 9, 10, 11 and 13, different types of effects occurred at the same site. Based on the collected EEEs, it has been possible to attribute the ESI 2007 intensity three localities. In sites 5, 6, 7, 14, 16, 17 and 18 the observed effects have been not sufficiently diagnostic, while in sites 2, 4 and 15 the effects are too sparse to assign an intensity to the corresponding locality. Background DTM (10 m spatial resolution) provided under COPERNICUS by the European Union and ESA, all rights reserved (produced using products © DLR e.V. (2014–2018) and © Airbus Defence and Space GmbH 2015).

The only possible evidence of primary effect was collected in the Hamallaj beach (site 13 in Fig. 8), where the local fishermen reported a seaward shift of the coastline. They testified that the rope, 30 m long, used to tie the boat to their hand winch, deep-rooted in the sandy beach, after the earthquake resulted too short to reach at sea to pull the boats ashore. They estimated that the shoreline had moved seaward of at least several meters, possibly 10.

By comparing the optical imagery acquired by satellite Sentinel-2A before (11 and 21 November 2019) and after the main shock (1 December 2019), a coastline progradation extending longitudinally for about 450 m south of the draining channel of the Hamallay beach might be inferred. This shift cannot be attributed to sea tides, because on December 1 the tide was higher than on November 11 (at 9:49 UTC, time of data acquisitions). Unfortunately, the 10 m spatial resolution of the Sentinel-2A scenes (post-event Google Earth imagery is still unavailable for the site) does not allow to precisely verify the actual amount of beach progradation indicated by the local fishermen. The warping of the Hamallaj beach area, that was uplifted >8 cm in the LOS (*ca*. 11 cm vertical) according to SAR interferometry (Figs 4 and 5), seems to be too modest to induce such a phenomenon. Moreover, right after the main shock, locally the Hamallaj beach appeared as in Fig. 9, as a consequence of lateral spreading, which might just explain the coastline shift.

Figure 9. Lateral spreading on the Hamallaj beach of Durres district. This photo has been published on 29 November 2019 by arbresh.info (http://www.arbresh.info/lajmet/shikoni-se-si-duket-plazhi-ne-durres/). Soon after the event, these features were washed out by storm sea waves and only a wide depressed area was left.

5.2 Secondary effects

Most of the secondary effects we observed during our field surveys are represented by liquefaction phenomena (sites 1, 3, 8, 9, 10, 11 and 18 in Fig. 8). Along the coast south of Durres, some buildings founded on the beach collapsed (sites 1 and 3) or were damaged also as a consequence of the liquefaction of sandy deposits. At site 3, the liquefaction was still well evident during the survey (Fig. 10).

Extensive liquefaction occurred also in the lagoons north of Durres (site 8; see also IGEWE 2019), near the mouth of Erzen river (sites 9 and 10) and around the village of Juba (site 11). In sites 9 and 10 we observed dozens of open ground fissures, up to tens of meters long, with associated liquefaction phenomena. In site 10 the most impressive fractures occurred, up to 50 cm large and with an observed depth in excess of 2 m. Along a NNE–SSW stretch of the Erzen River course, their total length was about 260 m. These fissures were clearly associated with the liquefaction and lateral

Figure 10. Liquefaction contributed to damage some buildings along the beach of Durres (site 3 of Fig. 8).

Figure 11. Site 9 of Fig. 8: Ground fracture (left-hand panel) induced by the Erzen river bank failure, with a 10–15 cm vertical throw lowering the side towards the river, and (right-hand panel) crack with ejected liquefied sandy silt. Cracks were up to tens of metres long.

spreading of the left river bank (Fig. 12d). In fact, they followed the U-shaped bank of the river and their vertical throw was constantly lowering the side toward the river. Other narrower (a few cm wide) fractures were characterized by the typical presence on both their edges of mounds of grey sandy silts. Figs 11 and 12 show some of the effects observed respectively in site 9 and 10.

Open ground fissures and fractures with associated liquefaction phenomena were widely observed also in the alluvial plain near the village of Juba (site 11 of Fig. 8). Some of these effects are shown in Fig. 13. Locally, the sandy alluvial deposits are buried under about 6 m of clayey silts and are water-saturated by the surficial aquifer. Ground cracks resulted up to 10–15 cm wide and up to tens of metres long. Liquefaction damaged some rural houses and, soon after the main shock, a mixture of water and sand was ejected up to a height of 1 m from a hole in the ground close to a water well (Fig. 13e).

About 50 m of the beach of Hamallaj (site 13 of Fig. 8) were affected by the lateral spread shown in Fig. 9. Even if, according to the interferometric data, that area was affected by uplift, suggesting the occurrence of possible warping phenomena, such effects can be more easily interpreted as local lateral spreading. Other liquefaction effects have been reported by the villagers of Tale, in the Lezha District (site 18 of Fig. 8), where ejections of water with sand from the ground occurred at a site located on a palaeo-course of the Mati river.

Also, few earthquake-induced landslides have been observed in sites 2, 4 and 15. Along the coastal road from Durres to south, a rockfall, with an estimated volume of 500–600 m^3, occurred along a near-vertical fractured slope, with layering according to slope direction (bedding strike 250/50°, Fig. 14). Indeed, the slide was not immediately triggered during the 26 November 2019, main event: two testimonies reported that it occurred 2 d after, presumably induced by aftershocks, or triggered by the heavy rain episode happened soon after the event, after having been weakened by the seismic shaking.

North of Durres, another small slide affected a steep instable clayey slope, shifting an old bunker several meters downward (site 4). The last evidence has been surveyed in the hilly reliefs east of Thumana, along a slope subject to surficial movements, where a reactivation occurred near the local outcrop of the

Figure 12. Site 10 of Fig. 8. Dozens of metres long fractures, opened up to 50 cm and associated with liquefaction, follow the left river bank of the Erzen River, affected by liquefaction and lateral spreading phenomena. (a) Panoramic view of one strand of these fractures. (b) Detail of a liquefaction conduct inside the fracture. (c) Side of a fracture showing the stratigraphy, with the soil above the clayey silts. (d) Lateral spreading of the Erzen River bank collapsed by liquefaction.

Figure 13. Liquefaction effects in the surroundings of Juba village. (a) Coalescent sand volcanoes; (b), (c) and (d) fractures with mounds of grey sandy silts on both rims. (e) Water and sand erupted up to a height of 1 m from a hole in the ground close to a water well. Site 11 of Fig. 8.

thrust front of the Albanides mountain range on the Tirana valley (site 15).

Seismic shaking caused also several typical ground fissures. We observed cracks along the rim of the southwestern side of Cape Bishtpalla (sites 5 and 6) and in the joints of limestones cropping out on the slopes of the Kruja Mountains east of Thumana (site 16), an arched fracture 30 m long and 2–10 cm wide cutting the road in front of the water pumping station of Hamallaj (site 12; Fig. 15) and several cracks cutting across the road near the water pumping station of Thumana (site 17).

Two hydrological anomalies were also reported. On the tip of Cape Bishtpalla (site 7), from a no longer productive deep methane gas well, a column of water and gas rose about 20 m lasting for days after the earthquake. It is worth noting that this unusual phenomenon had already occurred in the past, without correlation with strong seismic activities. Finally, in the territory of Thumana (site 14), the

Figure 14. Rock slide aside the road SH4 southward from Durres. Despite occurred after the heavy rains that followed the earthquake, presumably, it was triggered by seismic shaking. Site 2 of Fig. 8.

Figure 15. Ground fracture near the water pumping station of Hamallaj (site 12 of Fig. 8).

piezometric level of a water well changed from –6 m, a depth more or less constant over the last years, to ground level just after the earthquake.

5.3 Environmental seismic intensity (ESI)

Based on the collected earthquake environmental effects (EEEs), it has been possible to estimate the macroseismic intensity by applying the ESI scale (Michetti *et al.* 2007; Serva *et al.* 2016). The major tectonic evidence induced on the environment is the uplift >9 cm detected by interferometric analysis. Based on the latter and the lateral spreading effects, in the locality of Hamallaj the local I_{ESI} is slightly above VIII but smaller than IX (Fig. 8), lower than the estimated EMS98 value of IX (IGEWE 2019). At the mouth of the Erzen River, closer to the epicentral area, based on the fractures, liquefactions and lateral spreading phenomena, the I_{ESI} is also between VIII and IX. Towards the Juba village, I_{ESI} is VIII, according to observed fractures and liquefactions, as in site 8 of Fig. 8. Therefore, to the localities of Juba and Rrushkull, an I_{ESI} VIII–IX can be attributed, even in this case slightly lower than the EMS98 value. The effects collected along the Cape Bishtpalla cannot be considered diagnostic of any intensity value. An I_{ESI} at least VIII can be attributed to the locality of Durres, based on the liquefactions in site 3, while in site 1 it was not possible to survey the liquefaction effects because the site was heavily disrupted during the removal works of the collapsed building's rubble. Landslides in sites 2, 4 and 15 correspond to I_{ESI} V. The effects in sites 14, 16 and 17 do not provide diagnostic information, while in site 18 the collected testimony does not allow to estimate the intensity.

The few sites where it was possible to estimate an I_{ESI} value are insufficient to draw an Intensity field, but the information collected on the EEEs and the interferometric data allow to estimate the epicentral intensity of the earthquake. In fact, considering the areal distribution of the EEEs and the deformation estimated by the interferometry (supposing that some deformation occurred offshore too), the total affected area extends for about 800 km^2, corresponding to an epicentral intensity bracketed between VIII and IX (Michetti *et al.* 2007; Serva *et al.* 2016), in agreement with the I_{ESI} related to the ground uplift of at least 10 cm at Hamallaj.

6 DISCUSSION AND CONCLUSIONS

The M_w 6.4, 2019, earthquake has hit a region where recurring seismic events of moderate to strong magnitude (maximum estimated 6.6) are remembered in chronicles at Durres, the main port on the Greek side of the Adriatic along the ancient via Egnatia, since Roman times. In spite of this long record, spanning more than two millennia, the documentation is rather scanty, so that the actual epicentral area and the macroseismic intensities are often poorly constrained. According to Aliaj *et al.* (2004), the catalogue is complete for events of $M \geq 7$ since 1200 AD, which appears to be in agreement with the estimates for Greece and surroundings by Papazachos *et al.* (2000) of completeness for $M \geq 7.3$ since 1500 AD. The historical record in this region, but more in general in the Mediterranean basin suffers for the many sources lost by fire and looting until the XVI century. Thus, it has been impossible until now to attribute with certainty the known major events to a specific source. In general, they have been associated to the Durres Offshore Thrust (e.g. SHARE project, where it is named Lushnie Fault, Basili *et al.* 2013). The last event seems to confirm the correctness of this assumption. In fact, it likely occurred on a quite deep plane gently dipping east, at the base of the brittle crust, possibly representing the sole of the west-verging fold and thrust pile overlapping the undeformed foreland of the Adriatic–Apulian microplate that is imaged in the few available deep seismic lines. However, the latter show diverging interpretations, which we have tried to summarize and reconcile, where possible, in the section of Fig. 3. In this area the thrust runs offshore and seemingly does not reach the sea bottom. The upper tip of the last rupture, which has enucleated from the bottom of the brittle crust, is also offshore, despite quite close to the coast, as shown by the DInSAR deformation field and the Coulomb modelling, and rather deep (>14 km). The aftershocks distribution, as reported in the IGEWE bulletins, is quite puzzling, with a large scattering of the hypocentres, unable to define a preferential plane of rupture, extending down to 50 km, which would imply a questionable involvement of the whole crust.

Indeed, this event has caused a wide but modest uplift at surface and, perhaps, a rather small progradation of the shoreline reported by the local fishermen in a short stretch of coast near Hamallaj. However, the latter might be only a secondary effect, associated to the lateral spreading occurred nearby on the beach. The modelled Coulomb stress change does not show any significant contribution to stress loading in the major faults surrounding the 2019 rupture: Montenegro offshore thrust, Lezha transfer fault and Kruja thrust. Anyway, their state of stress is unknown and the scarce GPS monitoring stations are not yet able to characterize strain building on them. The 1979 Montenegro event of M_w 7.1 has likely unloaded the causative offshore thrust, but the seismic catalogue might not be fully representative of the seismic potential of the region, similarly to the case of the fault responsible for the 2019 earthquake. The poorly known Lezha fault, being the northern boundary of the epicentral area activated in 2019, may have a segmentation role in the seismic rupturing process between the frontal thrusts of Montenegro and Albania (Handy *et al.* 2020). Even less is known about the seismogenic potential of the Kruja thrust.

The 2019 earthquake has opened novel questions about the seismic and surface faulting hazards in northwestern Albania. Is the last earthquake the maximum potential event to be expected for the slipped fault? Can the latter, or another fault in the surroundings, generate a much stronger event and so a much larger uplift, with noticeable impact on the coastal structures and the local morphology, including the drainage pattern, which already shows evidence of ongoing ground deformation? Are the shallower back-thrusts activated by the motion of the main fault or do they move independently? What are their seismic potential and fault capability (i.e. their potential for displacement at or near the ground surface)? Are all the fault traces at/near surface well identified and mapped? What could be the hazard from coseismic folding? These questions need be answered with a thorough program of investigations, based on geological, geophysical and palaeoseismological methods, to reliably assess the seismic and surface faulting hazard in the densely urbanized coastal region and Tirana Valley. Such a study would also be crucial for the assessment of tsunami hazard in the Adriatic basin and the consequent NEAMTWS actions, being many active structures with estimated M_w >6 (e.g. SHARE project) located partially or completely offshore. According to the recent paper by Ganas *et al.* (2020), based on the observed GNSS shortening of the last event, the recurrence period for M 6+ events along the 2019 fault should be in the order of 150 yr. The historical record before the XIX century cannot confirm such an inference. Palaeoseismological studies would contribute verifying the actual seismic potential in terms of repeat intervals and maximum magnitude.

The macroseismic intensity assessed by IGEWE is IX EMS-98. The sparse geological effects of the earthquake have allowed to estimate a peak ESI 2007 intensity slightly >VIII, which appears more appropriate for such deep earthquake, also considering that several collapsed buildings were in poor structural conditions, while others were founded on recent saturated sand that was affected by liquefaction. The comparison of the EEEs and the resulting ESI intensity of the Durres earthquake with those of the few similar thrust events of the recent years in the Mediterranean Region (e.g. the M_w 5.9 and 5.7, 2012, Po Plain events in Italy, Di Manna *et al.* 2012; the M_w 5.6, 1998, Krn Mountains event in Slovenia, Gosar 2012; the M_w 5.1, 2011, Lorca event in Spain, Silva *et al.* 2015; and the M_w 6.8, 2003, Boumerdès earthquake in Algeria, Heddar *et al.* 2016), shows a good complementarity. The 2012 seismic sequence in the Po Plain was characterised by two main shocks with smaller magnitude but also much lower focal depth: M_w 5.9, focal depth 6 km and M_w 5.7, focal depth 10 km (Govoni *et al.* 2014). The subsurface geology of the epicentral area of the Po Plain sequence is quite similar to that of the Durres earthquake epicentral area, but with opposite vergence. In fact, the Po Plain frontal compressional structures, mostly buried under marine and continental clastic deposits, and backed by the Apennines orogenic belt, are overthrust northeastward on the Adria microplate (Govoni *et al.* 2014). In both areas, the geomorphological framework is characterized by a complex pattern of the drainage and palaeodrainage lines, strongly influenced by the ongoing activity of the buried fold and thrust belt (Di Manna *et al.* 2012, and references therein).

The similar geological and geomorphological conditions led to EEEs very similar to those of 2019, that is comparable uplift (up

to about 20 cm for the shallower Po plain sequence; Bignami *et al.* 2012) and widespread liquefaction phenomena. Moreover, the long and wide fracture system occurred at the mouth of the Erzen river (site 10) is very similar to the set of SW–NE fractures (San Carlo and Mirabello areas) resulting from liquefaction and lateral spreading, described for a length of about 6.5 km as a major effect of the 2012 Po Plain event. In 2012, the distribution of ground effects led to estimate an intensity VIII on the ESI 2007 scale, even if the impressive lateral spread might have suggested a slightly higher peak intensity (Di Manna *et al.* 2012). Of course, the flatness of the epicentral areas has triggered very little landslides or rock falls, which are, instead, the most common EEEs in mountain areas, as occurred during the M_w 5.6, 1998, Krn Mountains event in Slovenia (Gosar 2012) and the M_w 5.1, 2011, Lorca event in Spain (Silva *et al.* 2015). As well, another reverse faulting event hardly comparable to the Durres event was the M_w 6.8, 2003, Boumerdès earthquake in Algeria (Heddar *et al.* 2016), with a hypocentre 10 km deep. Here, a major primary effect was the uplift of a wide costal area reaching 0.55–0.7 m along a 40-km-long section centred in the epicentre area (Meghraoui *et al.* 2004), causing damages to the Zemmouri and Algiers harbours. Surface faulting very likely took place but was not observed being the rupture offshore. Thus, the effects of the 2019 earthquake are relevant for complementing the catalogue of EEEs and ESI scale estimates and the relationship between magnitude and ESI intensity of Papanikolaou & Melaki (2017) for reverse faulting earthquakes in the Mediterranean Region, confirming at the same time its validity despite the scarcity of comprised reverse faulting events, since it properly predicts an intensity VIII–IX for an M_w 6.4 earthquake.

In conclusion, this paper has been devoted to describe the main effects of the 2019 earthquake within the frame of the seismotectonic setting of the region, to contribute assessing the intensity field by means of the ESI 2007 scale and to try identifying and characterizing the most likely seismogenic source. The obtained results, seen in the tectonic framework resulting from the now available studies show that the in-depth understanding and characterization of each potential seismogenic source necessary for a proper seismic hazard assessment is still to come and must be a near future objective.

ONLINE RESOURCES

The data underlying this article are all freely available in the following repositories and websites, lastly accessed in October 2020:

CFTIMed: http://storing.ingv.it/cfti/cfti5/
GCMT: https://www.globalcmt.org/
EMSC (moment tensors 2019 earthquake): https://www.emsc-csem.org/Earthquake/mtfull.php?id=807751&year=2019;INFO
IGEWE seismological bulletins: (https://www.geo.edu.al/newweb/?fq=sizmobuletinet&gj=gj2&kid=36)
ISC: http://www.isc.ac.uk/iscbulletin/search/catalogue/
http://www.isc.ac.uk/iscbulletin/search/fmechanisms/
ISIDE: http://iside.rm.ingv.it/en/search
Plutarch, Life of Cicero: http://penelope.uchicago.edu/Thayer/E/Roman/Texts/Plutarch/Lives/Cicero*.html
RCMT: http://rcmt2.bo.ingv.it/
SHARE (European Database of Seismogenic Faults): http://diss.rm.ingv.it/share-edsf/
SHEEC: https://www.emidius.eu/SHEEC/catalogue/
ASIG geoportal (several WMS resources, including the Geological Map): https://geoportal.asig.gov.al/en/data
USGS (Coulomb software): https://earthquake.usgs.gov/research/software/coulomb/
NEAMTWS (Tsunami Information Center): http://neamtic.ioc-unesco.org/index.php?option=com_content&view=article&id=216&Itemid=472

ACKNOWLEDGEMENTS

This manuscript has largely benefited from the careful review by Klaus Reicherter and an anonymous referee; we warmly thank both of them. The Italian colleagues are grateful to the Albanian people for their friendly welcome and generous hospitality even in the difficulties of the earthquake. A warm thanks to Kostandin and his wife for their friendliness and for sharing their homemade *raki*. A special thanks to our guide Klodian who has wisely driven us until nightfall along the muddy meanders near the mouth of the Erzen River.

A special appreciation goes to the developers of the valuable free software QGIS (GIS system) and Coulomb3 and to all people who allow researchers to obtain open and timely access to seismological and geodetic data.

REFERENCES

Aliaj, S., 2000. Neotectonics and seismicity in Albania, in *Geology of Albania,* pp. 135–178, eds Meco, S., Aliaj, S. & Turku, I., Gebruder Borntrager, Beitrage zur regionalen Geologie der Erde, **28**.

Aliaj, S., 2006. The Albanian Orogen: convergence zone between Eurasia and the Adria Microplate, in *The Adria Microplate: GPS Geodesy,* Vol. 61, Tectonics and Hazards, NATO Sciences, Series IV: Earth and Environmental Sciences, pp. 133–149, eds Pinter, N., Grenerczy, G., Weber, J., Stein, S. & Medak, D., Springer.

Aliaj, S., Adams, J., Halchuk, S., Sulstarova, E., Peci, V. & Muco, B., 2004. Probabilistic seismic hazard maps for Albania, in *Proceedings of the 13th World Conference on Earthquake Engineering*, Vancouver, B. C., Canada, August 1–6, 2004, Paper No. 2469.

Aliaj, S., Koçiu, S., Muço, B. & Sulstarova, E., 2010. *Seismicity, Seismotectonics and Seismic Hazard Assessment in Albania,* Academy of Sciences of Albania, pp. 98.

Aliaj, S., Sulstarova, E., Muço, B. & Koçiu, S., 2000. *Seismotectonic Map of Albania in Scale 1:500,000,* Seismological Institute, Tirana.

Argnani, A., 2013. The influence of Mesozoic palaeogeography on the variations in structural style along the front of the Albanide thrust-and-fold belt, *Ital. J. Geosci.,* **132,** 175–185.

Aubouin, J., Blanchet, R., Cadet, J.P., Celet, P., Charvet, J., Chorowicz, J., Cousin, M. & Rampnoux, J., 1970. Essai sur la géologie des Dinarides. *Bull. Soc. Géol. De France,* **7**(6), 1060–1095.

Basili, R. *et al.* 2013. The European Database of Seismogenic Faults (EDSF) compiled in the framework of the Project SHARE. http://diss.rm.ingv.it/share-edsf/, doi: 10.6092/INGV.IT-SHARE-EDSF.

Bega, Z., 2013a. Deep seated platform carbonate reservoirs as new hydrocarbon plays in the NW Albania–Montenegro segment of the Adriatic Region, in *Presentation at the AAPG Conference*, Barcelona April 8–10, 2013.

Bega, Z., 2013b. Hydrocarbon exploration opportunities in Albania: A review of recent exploration activities, in *Paper presented at the 7th Balkan - Geophysical Society Congress, Conference and Technical Exhibition*, 7–10 October, Tirana.

Bega, Z. & Soto, J.I., 2017. The Ionian fold-and-thrust belt in Central and Southern Albania - a petroleum province with Triassic evaporates, in *Permo-Triassic salt provinces of Europe, North Africa and the Atlantic Margins - Tectonics and Hydrocarbon Potential,* pp. 517–542, eds Soto, J. I., Flinch, J. & Tari, G., Elsevier Inc.

Benetatos, C. & Kiratzi, A., 2006. Finite-fault slip models for the 15 April 1979 (M-W 7.1) Montenegro earthquake and its strongest aftershock of 24 May 1979 (M-W 6.2), *Tectonophysics,* **421** (1–2), 129–143.

Biermanns, P., Schmitz, B., Ustaszewski, K. & Reicherter, K., 2018. Tectonic geomorphology and Quaternary landscape development in the Albania-Montenegro border region: An inventory. *Geomorphology,* **326,** 116–131. https://doi.org/10.1016/j.geomorph.2018.09.014.

Bignami, C. *et al.* 2012. Coseismic deformation pattern of the Emilia 2012 seismic sequence imaged by Radarsat-1 interferometry. *Ann. Geophys.,* **55**(4), doi:10.4401/ag-6157.

Braun, A. & Veci, L., 2020. Sentinel-1 Toolbox: TOPS Interferometry Tutorial, Revision January 2020, ESA, *SkyWatch Space Applications,* 25. http://step.esa.int/docs/tutorials/S1TBX%20TOPSAR%20Interferometry%20with%20Sentinel-1%20Tutorial_v2.pdf

Caporali, A., Floris, M., Chen, X., Nurce, B., Bertocco, M. & Zurutuza, J., 2020. The November 2019 Seismic Sequence in Albania: geodetic constraints and fault interaction, *Remote Sens.,* **12**(5), 846.

D'Agostino, N., Avallone, A., Cheloni, D., D'Anastasio, E., Mantenuto, S. & Selvaggi, G., 2008. Active tectonics of the Adriatic region from GPS and earthquake slip vectors, *J. geophys. Res.,* **113,** B12413.

DeCelles, P.G. & Giles, K.A., 1996. Foreland basin systems, *Basin Res.,* **8,** 105–123.

Di Manna, P. *et al.* 2012. The geological effects induced by the 2012 seismic sequence in Emilia: implications for seismic hazard assessment in the Po Plain. *Ann. Geophys.,* **55**(4), 697–703.

Doglioni, C., 1991. A proposal for the kinematic modelling of W-dipping subductions – possible applications to the Tyrrhenian-Apennines system. *Terra Nova,* **3,** 423–434.

Doglioni, C., Carminati, E., Cuffaro, M. & Scrocca, D., 2007. Subduction kinematics and dynamic constraints, *Earth-Sci. Rev.,* **83**(3-4), 125–175.

Dumurdzanov, N., Serafimovski, T. & Burchfiel, B.C., 2005. Cenozoic tectonics of Macedonia and its relation to the South Balkan extensional regime, *Geosphere,* **1,** 1–22, https://doi.org/10.1130/GES00006.1.

Elsie, R., 2003. *Early Albania, a Reader of Historical Texts, 11th - 17th Centuries,* Wiesbaden, pp. 12–13. http://www.albanianhistory.net/1267_Pachymeres/index.html.

Fantoni, R. & Franciosi, R., 2010. Tectono-sedimentary setting of the Po Plain and Adriatic foreland, *Rend. Fis. Acc. Lincei,* **21,** S197–S209.

Frasheri, A., Bushati, S. & Bare, V., 2009. Geophysical outlook on structure of the Albanides, *J. Balkan Geophys. Soc.,* **12**(1), 9–30.

Ganas, A., Elias, P., Briole, P., Cannavo, F., Valkaniotis, S., Tsironi, V. & Partheniou, E.I., 2020. Ground deformation and seismic fault model of the M6.4 Durres (Albania) Nov. 26, 2019 Earthquake, based on GNSS/INSAR observations. *Geosciences,* **10**(6), 210. https://doi.org/10.3390/geosciences10060210.

Gosar, A., 2012. Application of Environmental Seismic Intensity scale (ESI 2007) to Krn Mountains 1998 Mw = 5.6 earthquake (NW Slovenia) with emphasis on rockfalls, *Nat. Hazards Earth Syst. Sci.,* **12,** 1659–1670.

Govoni, A. *et al.* 2014. The 2012 Emilia seismic sequence (Northern Italy): Imaging the thrust fault system by accurate aftershock location. *Tectonophysics,* **622,** 44–55.

Grad, M. & Tiira, T. ESC Working Group, 2009. The Moho depth map of the European Plate, *Geophys. J. Int.,* **176**(1), 279–292.

Grünthal, G., (Ed.), 1998. European Macroseismic Scale 1998. European Seismological Commission, Subcommission on Engineering Seismology, Working Group Macroseismic Scales, *Cahiers du Centre Européen de Géodynamique et de Séismologie,* **15,** 99. Luxemburg.

Guidoboni, E. *et al.* 2019. CFTI5Med, the new release of the catalogue of strong earthquakes in Italy and in the Mediterranean area, *Scientific Data,* **6,** doi:10.1038/s41597-019-0091-9.

Guzmán, O., Mugnier, J.L., Vassallo, R., Koçi, R. & Jouanne, F., 2013. Vertical slip rates of active faults of southern Albania inferred from river terraces, *Ann. Geophys.,* **56**(6), S0676, doi:10.4401/ag-6218.

Handy, M.R., Giese, J., Schmid, S.M., Pleuger, J., Spakman, W., Onuzi, K. & Ustaszewski, K., 2019. Coupled crust-mantle response to slab tearing, bending, and rollback along the Dinaride-Hellenide orogen, *Tectonics,* **38,** doi: 10.1029/ 2019TC005524.

Handy, M.R., Stefan, M., Schmid, S.M. & Briole, P., 2020. The M 6.4 Albanian earthquake of Nov. 26, 2019 and its relation to structures at the Dinarides-Hellenides junctions, EGU2020-5409, *EGU General Assembly* **2020,** https://doi.org/10.5194/egusphere-egu2020-5409.

Heddar, A., Beldjoudi, H., Authemayou, C., SiBachir, R., Yelles, C.A & Boudiaf, A., 2016. Use of the ESI-2007 scale to evaluate the 2003 Boumerdès earthquake (North Algeria). *Ann. Geophys.,* **59,** doi:10.4401/ag-6926.

Hoffmann, N., Reicherter, K., Fernández-Steeger, T. & Grützner, C., 2010. Evolution of ancient Lake Ohrid: a tectonic perspective. *Biogeosciences,* **7,** 3377–3386.

Hoxha, L., 2020. On the presence of the strike slip faults in the northern Albania, *Geol. Soc. Am. Abstr. Prog.,* **52**(2), doi:10.1130/abs/2020SE-343221.

IGEWE, 2019. Monthly Bulletin of Seismology, Nr. 5, November 2019. Universiteti Politeknik i Tiranës, Institute of Geosciences, Energy, Water and Environment, Tirana, 336 p. ISSN: 2664–410X (in Albanese, with summary in English).

Jardin, A., Roure, F. & Nikolla, L., 2011. Subsalt depth seismic imaging and structural interpretation in Dumre area, Albania, *Oil Gas Sci. Technol.,* **66,** 911–929.

Jouanne, F. *et al.* 2012. GPS constraints on current tectonics of Albania, *Tectonophysics,* **554–557,** 50–62.

Karnik, V., 1969. *Seismicity of the European Area,* Part 1, D. Riedel Publishing Co., pp. 364.

Kilias, A., Tranos, M.D., Mountrakis, D., Shallo, M., Marto, A. & Turku, I., 2001. Geometry and kinematics of deformation in the Albanian orogenic belt during the Tertiary, *J. Geodyn.,* **31**(2), 169–187.

Kiratzi, A. & Dimakis, E., 2013. Focal mechanisms and slip models of moderate size earthquakes in Albania and adjacent countries, *Italian Journal of Geosciences,* **132**(2), 186–193.

Lacombe, O., Malandain, J., Vilasi, N., Amrouch, K. & Roure, F., 2009. From paleostress to paleoburial in fold-thrust belts: Preliminary results from calcite twin analysis in the Outer Albanides, *Tectonophysics,* **475,** 128–141.

Lekkas, E., Mavroulis, S., Filis, C. & Carydis, P., 2019a. The September 21, 2019 Mw 5.6 Durres (Albania) earthquake, in *Newsletter of Environmental, Disaster and Crises Management Strategies,* **13,** 1–64, National and Kapodistrian University of Athens, ISSN 2653–9454.

Lekkas, E., Mavroulis, S., Papa, D. & Carydis, P. 2019b. The November 26, 2019 Mw 6.4 Durres (Albania) earthquake, in *Newsletter of Environmental, Disaster and Crises Management Strategies,* **15,** 1–80, National and Kapodistrian University of Athens, ISSN 2653–9454.

Leonard, M., 2014. Self-consistent earthquake fault-scaling relations: Update and extension to stable continental strike-slip faults. *Bull. seism. Soc. Am.,* **104,** 2953–2965.

Lule, A. & Naza, S., 2020. The geological setting of Durrës - Rodon Region in Albania, *J. Int. Envir. Appl. Sci.,* **15**(2), 41–47.

Makropoulos, K., Kaviris, G. & Kouskouna, V., 2012. An updated and extended earthquake catalogue for Greece and adjacent areas since 1900, *Nat. Hazards Earth Syst. Sci.,* **12,** 1425–1430.

Mantovani, E., Viti, M., Babbucci, D., Albarello, D., Cenni, N. & Vannucchi, A., 2010. Long-term earthquake triggering in the Southern and Northern Apennines, *J. Seismol.,* **14,** 53–65.

Meghraoui, M., *et al.*, 2004. Coastal uplift and thrust faulting associated with the Mw = 6.8 Zemmouri (Algeria) earthquake of 21 May, 2003, *Geophys. Res. Lett.,* **31**(8):L19605, doi:10.1029/2004GL020466.

Meço, S. & Aliaj, S., 2000. *Geology of Albania,* pp. 246, Gebruder Borntraeger.

Michetti, A.M. *et al.* 2007. Intensity scale ESI 2007, in *Mem. Descr. Carta Geologica d'Italia,* Vol. **LXXIV,** eds Guerrieri, L. & Vittori, E., Servizio Geologico d'Italia, Dipartimento Difesa del Suolo, APAT, Rome, Italy.

Mihailovic, D.J., 1951. *Catalogue des Tremblements de Terre Epiro-Albanais*. Archive Seismologique de L'Institut seismologique de Beograd, Zagreb.

Naço, P., Kaza, G., Doda, V., Vinçani, F. & Cara, F., 2014. Contribution of the reflected waves method in structural modeling of Albanides, *J. Eng. Res. Appl.,* **4,** 299–307.

Nikolla, L., Kuneshka, M., Ademi, F. & Bejtaj, K., 2002. *Development and Structural Styles of Albanides,* www.akbn.gov.al.

Ormeni, R., Fundo, A., Daja, S. & Doda, V., 2013. Moderate earthquakes in Albania during 2009 and their associated seismogenic zones, *Ital. J. Geosci.,* **132**(2), 203–212.

Papadopoulos, G.A., Agalos, A., Carydis, P., Lekkas, E., Mavroulis, S. & Triantafyllou, I., 2020. The 26 November 2019 Mw 6.4 Albania destructive earthquake. *Seismol. Res. Lett.,* **XX,** 1–10, doi: 10.1785/0220200207.

Papanikolaou, I. & Melaki, M., 2017. The Environmental Seismic Intensity Scale (ESI 2007) in Greece, addition of new events and its relationship with magnitude in Greece and the Mediterranean; preliminary attenuation relationships. *Quater. Int.,* **451,** 37–55.

Papazachos, B.C., Comninakis, P.E., Karakaisis, G.F., Karakostas, V.G., Papaioannou, Ch.A., Papazachos, C.B. & Scordilis, E.M., 2000. A catalogue of earthquakes in Greece and surrounding area for the period 550BC–1999. *Publ. Geophys. Lab. Aristotle Univ. of Thessaloniki* **1,** 338.

Papazachos, B.C. & Papazachou, C., 2003. *The Earthquakes of Greece*. Ziti Publications, 286 pp. (in Greek).

Pondrelli, S., 2002. European-Mediterranean Regional Centroid-Moment Tensors Catalog (RCMT) [Data set]. *Istituto Nazionale di Geofisica e Vulcanologia (INGV)*. https://doi.org/10.13127/rcmt/euromed.

Reicherter, K., Hoffmann, N., Lindhorst, K., Krastel, S., Fernández-Steeger, T., Christoph Grützner, C. & Wiatr, T., 2011. Active basins and neotectonics: morphotectonics of the Lake Ohrid Basin (FYROM and Albania), *Z. dt. Ges. Geowiss.,* **162**(2), 217–234.

Roure, F., Nazaj, S., Mushka, K., Fili, I., Cadet, J.P. & Bonneau, M., 2004. Kinematic evolution and petroleum systems: an appraisal of the outer Albanides, in *Thrust Tectonics and Hydrocarbon Systems,* pp. 474–493, ed. McClay, K.R., **82,** AAPG Memoir.

Roure, F., Prenjasi, E. & Xhafa, Z., 1995b. Trip #7, Albania: Petroleum geology of the Albanian thrust belt, in *Proceedings of the AAPG International Conference,* Nice, pp. 50.

Roure, F., Sadiku, U. & Valbona, U., 1995a. *Petroleum Geology of the Albanian Foothills,* AAPG Nice, Guide-Book, 100.

Roure, F. & Sassi, W., 1995. Kinematic of deformation and petroleum potential appraisal in Neogene fore- land fold-and-thrust belt systems, *Petrol. Geosci.,* **1,** 253–269.

Schmid, S.M. *et al.* 2008. The Alpine-Carpathian-Dinaridic orogenic system: correlation and evolution of tectonic units, *Swiss J. Geosci.,* **101**(1), 139–183.

Schmid, S.M. *et al.* 2019. Tectonic units of the Alpine collision zone between Eastern Alps and western Turkey, *Gondwana Res.,* https://doi.org/10.1016/j.gr.2019.07.005.

Serva, L. *et al.* 2016. Earthquake hazard and the Environmental Seismic Intensity (ESI) scale, *Pure appl. Geophys.,* **173**(5), 1479–1515.

Silva, P.G., Perez-Lopez, R., Rodriguez-Pascua, M., Roquero, E., Giner-Robles, J., Huerta, P., Martínez-Graña, A. & Azcárate, T., 2015. Macroseismic analysis of slope movements triggered by the 2011 Lorca Earthquake (Mw 5.1): application of the ESI-07 scale. *Geogaceta,* **57,** 35–38.

Skrami, J., 2001. Structural and neotectonic features of the Periadriatic Depression (Albania) detected by seismic interpretation, *Bull. Geol. Soc. Greece,* **34**(4), 1601–1609.

Stipčević, J., Herak, M., Molinari, I., Dasović, I., Tkalčić, H. & Gosar, A., 2020. Crustal thickness beneath the Dinarides and surrounding areas from receiver functions. *Am. Geophys. Un.,* **39**(3), doi:10.1029/2019TC005872.

Stucchi, M. *et al.* 2013. The SHARE European Earthquake Catalogue (SHEEC) 1000–1899, *J. Seismol.,* **17,** 523–544.

Sulstarova, E. & Kociu, S., 1975. The catalogue of Albanian earthquakes, *Botim i Qendres Sizmologjike,* Tirane, 223 pp.

Toda, S., Stein, R.S., Sevilgen, V. & Lin, J., 2011. Coulomb 3.3 Graphic-rich deformation and stress-change software for earthquake, tectonic, and volcano research and teaching, user guide, U.S. Geological Survey Open-File Report, 2011-1060, pp. 1–63, http://pubs.usgs.gov/of/2011/1060/.

Velaj, T., 2011. Tectonic style in Western Albania thrust belt and its implications on hydrocarbon exploration, *AAPG Search Dis. Art.,* 123–148.

Velaj, T., 2015a. The structural style and the hydrocarbon exploration of the subthrust in the Berati Anticlinal Belt, Albania, *J. Petrol. Explor. Product. Technol.,* **5,** 123–145.

Velaj, T., 2015b. New ideas on the tectonic of the Kurveleshi anticlinal belt in Albania and the perspective for exploration in its subthrust, *Petroleum,* **1**(4), 269–288.

Velaj, T., Davison, I., Serjani, A. & Alsop, I., 1999. Thrust tectonics and the role of evaporites in the Ionian Zone of the Albanides, *AAPG Bull.,* **83**(9), 1408–1425.

Viti, M., Mantovani, E., Babbucci, D., Cenni, N. & Tamburelli, C., 2015. Where the next strong earthquake in the Italian peninsula? Insights by a deterministic approach, *Boll. Geof. Teorica Appl.,* **56**(2), 329–350.

Wells, D.L. & Coppersmith, K.J., 1994. New empirical relationships among magnitude, rupture length, rupture width, rupture area, and surface displacement, *Bull. seism. Soc. Am.,* **84,** 974–1002.

Xhomo, A. *et al.* 1999. Geological map of Albania (1:200.000). Tirana: Ministry of Industry and Energy, Ministry of Education and Science, Albanien Geological Survey, AlpPetrol, Polytechnical University of Tirana.